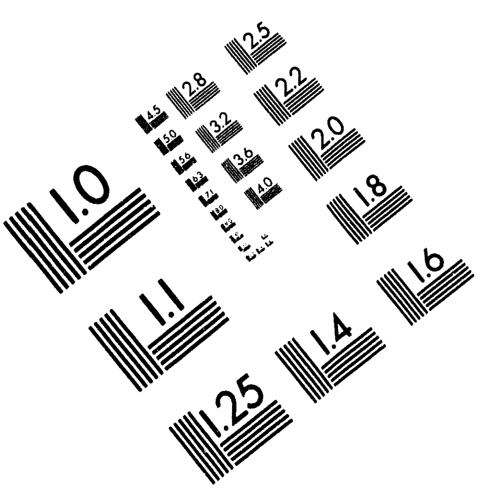

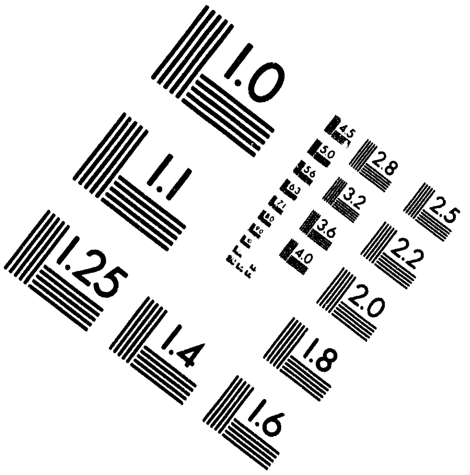

AIIM

Association for Information and Image Management

1100 Wayne Avenue, Suite 1100
Silver Spring, Maryland 20910

301/587-8202

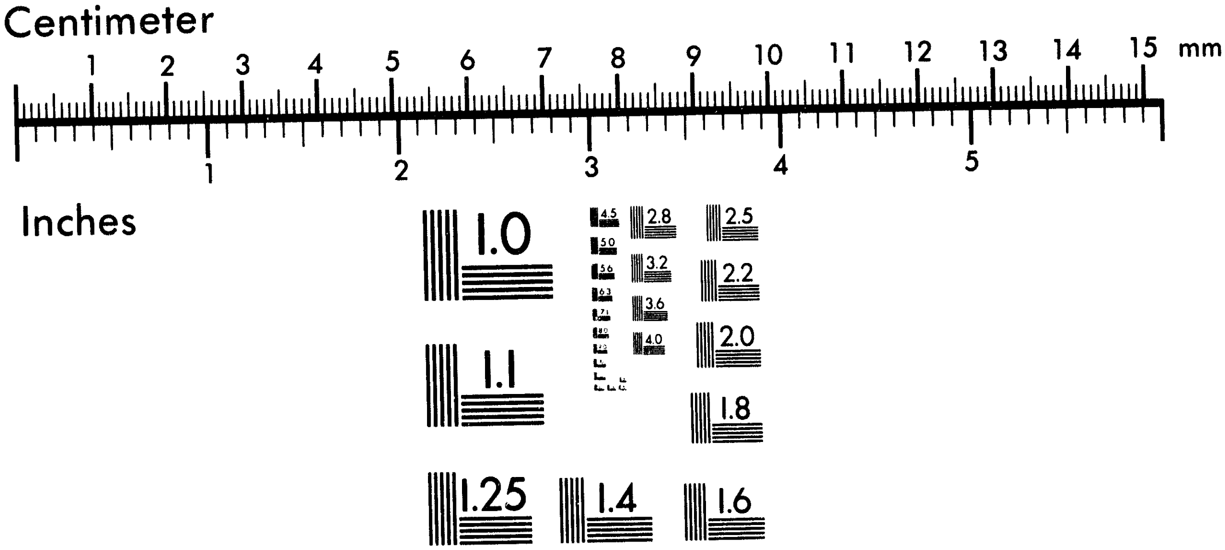

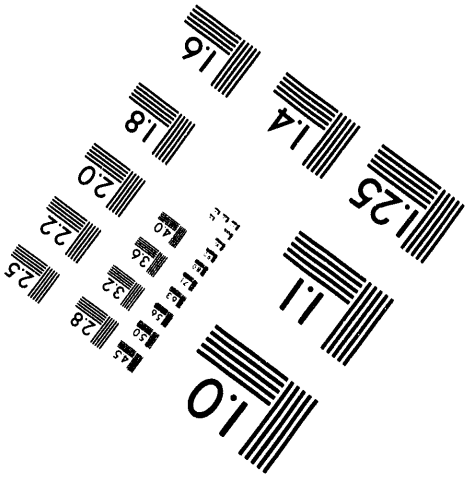

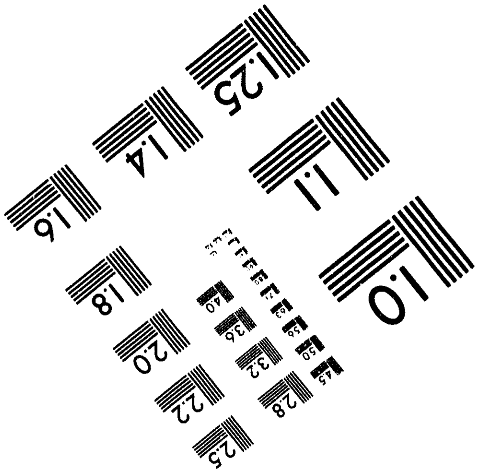

MANUFACTURED TO AIIM STANDARDS
BY APPLIED IMAGE, INC.

1 of 1

Conf-9410132--1

SAND94-1617C

MICROCONTAMINATION DETECTION USING HEAVY ION BACKSCATTERING SPECTROMETRY.*

James A. Knapp, James C. Banks, Sandia National Laboratories, and Alain C. Diebold, SEMATECH.

INTRODUCTION

Heavy Ion Backscattering Spectrometry (HIBS) is a new ion beam analysis tool using heavy, low-energy ions in backscattering mode which can detect very low levels of surface contamination.[1-5] By taking advantage of the greatly increased scattering cross-section for such ion beams and eliminating unwanted substrate scattering with a thin carbon foil, our research system has achieved a sensitivity ranging from ~$5x10^{10}$ atoms/cm^2 for Fe to ~$1x10^9$ atoms/cm^2 for Au on Si, without preconcentration. A stand-alone HIBS prototype now under construction in collaboration with SEMATECH is expected to achieve detection limits of ~$5x10^9$ atoms/cm^2 for Fe and ~$1x10^8$ atoms/cm^2 for Au on Si, again without preconcentration. Since HIBS is standardless and has no matrix effects, it will be useful not only as a standalone tool, but also for benchmarking standards for other tools.

This conference is testimony to the importance of controlling contamination in microelectronics manufacturing. By the turn of the century, very large scale integrated circuit processing is expected to require contamination levels well below $1x10^9$ atoms/cm^2 in both starting materials and introduced by processing.[6] One of the most sensitive of existing general-purpose tools is Total reflection X-Ray Fluorescence (TXRF), which can detect ~$1x10^{10}$ atoms/cm^2 levels of some elements such as Fe and Cu, but for many elements it is limited to $1x10^{12}$ atoms/cm^2 or worse. TXRF can achieve a sensitivity of 10^8 atoms/cm^2 through the use of synchrotron radiation or via pre-concentration using Vapor Phase Decomposition (VPD).[7] HIBS, on the other hand, provides an ion beam analysis capability with the potential for providing similar sensitivity at medium Z and higher sensitivity at larger Z, all without pre-concentration or matrix effects.

We have developed a Time-of-Flight (TOF) ion detector for use with HIBS, optimizing the design to achieve as high a sensitivity as possible.[3-5] The present research prototype of this detector, mounted in a chamber in our Ion Beam Materials Research Laboratory, has achieved a sensitivity of ~$1x10^9$ atoms/cm^2 for Au on Si and ~$5x10^{10}$ for Fe. These sensitivity numbers are for a single detector. The design allows up to three detectors to be arrayed around the analysis beam to give correspondingly higher sensitivity. The HIBS beta system being built under a Cooperative Research and Development Agreement (CRADA) with SEMATECH

---

* Portions of this work were done at Sandia National Laboratories and supported by the United States Department of Energy under Contract DE-AC04-94AL85000.

will have such an arrangement of three parallel detectors, along with a larger beam spot, which also improves the sensitivity.

DETECTOR DESIGN

HIBS, which is a technique useful primarily for detecting heavy impurities on a light substrate, is a modification of Rutherford backscattering spectrometry (RBS) using low energy, heavy mass ion beams. RBS is typically performed using a 1-2 MeV He^+ ion beam for the analysis, resulting in a sensitivity of $\sim 10^{13}$ atoms/cm^2 to impurities at or near the surface, limited by system noise. In a backscattering experiment the number of particles scattered in the direction of the detector determines the yield of counts from that particular target, and for the proper energy range is given by Rutherford's formula[8], as transformed from center-of-mass to a laboratory frame of reference differential scattering cross-section by Darwin[9]:

$$\frac{d\sigma}{d\Omega} = \left(\frac{Z_1 Z_2 e^2}{2E\sin^2\theta}\right)^2 \frac{\left\{\cos\theta + \left[1 - \left(\frac{M_1}{M_2}\sin\theta\right)^2\right]^{\frac{1}{2}}\right\}^2}{\left[1 - \left(\frac{M_1}{M_2}\sin\theta\right)^2\right]^{\frac{1}{2}}} \qquad \text{(eq. 1)}$$

where Z_1 and Z_2 are the atomic numbers of the projectile and target atom, e is electron charge, and E is the energy of the particle immediately before scattering. The average scattering cross section, σ, is defined as

$$\sigma = \frac{1}{\Omega}\int \frac{d\sigma}{d\Omega}\, d\Omega \qquad \text{(eq. 2)}$$

where the integration is over Ω, the finite solid angle spanned by the detector.

Examination of Eq. 1 will show that the backscattering yield is proportional to the square of the atomic number of the analyzing beam and inversely proportional to the square of its energy, so an enhanced yield can be obtained by using a higher Z ion beam at lower energy. Although this yield enhancement is well known, it is not widely exploited because pileup due to yield from the lower mass substrate overwhelms the signal from ions scattered by trace surface impurities. (Pileup occurs in an energy detector when multiple low-energy signals arrive simultaneously at a detector, such that they are indistinguishable from a single, higher-energy event). The key innovation in HIBS is that pileup is substantially reduced by a simple ranging foil in front of the detector which allows only particles backscattered from species heavier than the substrate to reach the detector.

Our original implementation of HIBS used a standard surface barrier particle energy detector (SBD) with a C foil placed in front of the detector.[1,2,5] The primary advantages of the SBD approach are low cost and simplicity. Limitations in this approach are due to the relatively poor resolution of SBD detectors in this energy regime and the dead layer (inactive region) in the surface of the detector. These in turn led to poor mass resolution; it was very difficult, for example, to separate contributions from Fe and Cu, if both were present. By changing to a TOF detector, we obtain substantially better energy and mass resolution at the cost of greater complexity. TOF detection schemes for ion beam analyses have typically been optimized for good energy and mass resolution, with very small solid angles.[10] For the trace contamination analyses of HIBS, a larger solid angle was desirable, while energy resolution was not as critical. The advantages of TOF detection for this application include the ability to detect lower energy particles (with no dead layer in the detector), which in turn allows a lower analysis beam energy and hence higher sensitivity. In addition, because the resulting spectrum is a time spectrum, the contributions from different masses are separated more widely at lower mass, which is the reverse of the situation for an energy spectrum. Thus the mass resolution is enhanced at lower mass, which is an advantage for application to problems of interest to the microelectronics community. The disadvantages of TOF ion detection are the greater complexity of the detector and its electronics, and the difficulty in achieving a large solid angle (needed for high sensitivity).

The research prototype TOF-HIBS detector is shown in Fig. 1, with its large area stop detector and a relatively short 12 cm. flight path used to maximize solid angle, while keeping energy resolution within acceptable bounds.[5] The ion beam is 2 mm in diameter. The samples in the research chamber are mounted on a 6 position, 2-axis goniometer, with only high purity Al or low Z material used for mounting. As with the SBD approach to HIBS, a carbon foil is used to block particles backscattered from the substrate, but it now also provides an electron timing start pulse. The TOF detector system consists of two event timing detectors. As backscattered ions pass through the thin carbon foil, they produce secondary electrons which are accelerated through an adjacent grid and detected by an electron microchannel plate (MCP) assembly. The ions continue their flight until stopped in the ion MCP, giving a second timing pulse.

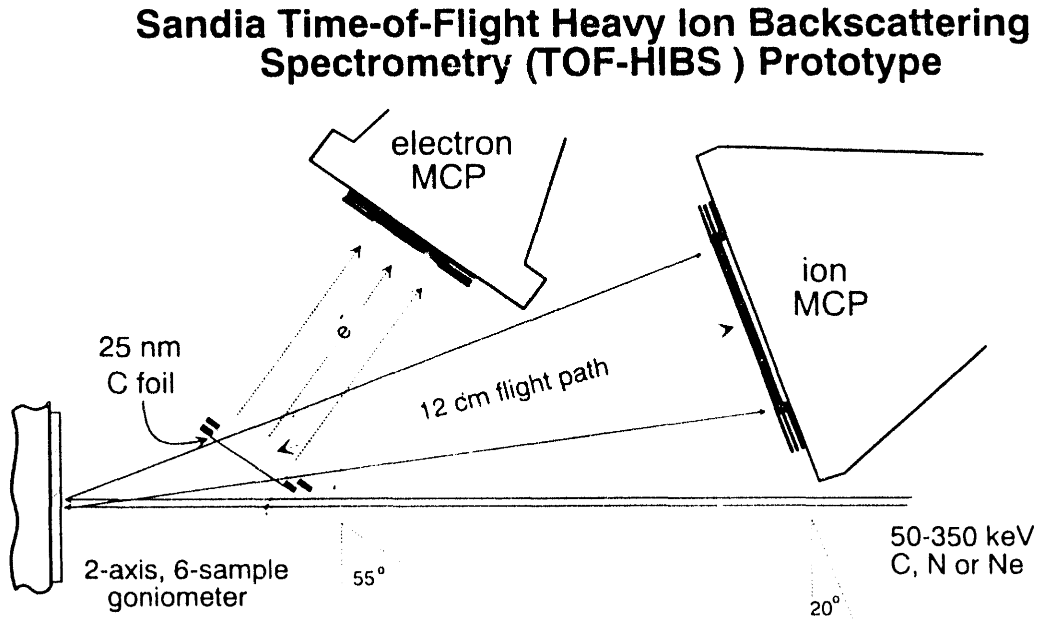

Sandia Time-of-Flight Heavy Ion Backscattering Spectrometry (TOF-HIBS) Prototype

Figure 1. Schematic of the research prototype Time-of-Flight HIBS detector.

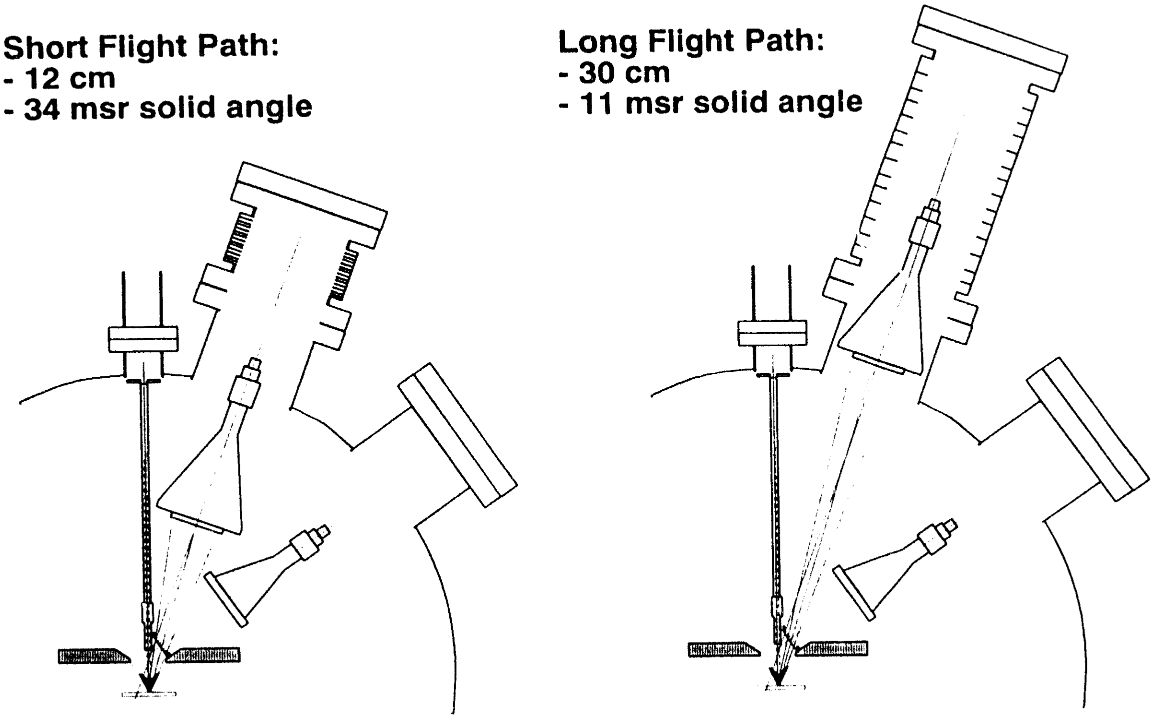
Short Flight Path:
- 12 cm
- 34 msr solid angle

Long Flight Path:
- 30 cm
- 11 msr solid angle

Figure 2. Schematic of the two configurations of the detector. The short flight path, high solid angle is for high sensitivity, the primary application; the long flight path configuration gives higher depth and mass resolution at the cost of sensitivity.

Since it was desirable to maximize the solid angle for improving sensitivity, the angle subtended by the ion MCP is relatively large, which leads to kinematic broadening. That is, the kinematic factor (energy) for backscattering from each mass changes from one side of the plate to the other. The angles of both the foil and the ion MCP were chosen by computer simulation during the design phase to minimize this broadening. The foil and associated electron MCP are at 55° relative to the sample plane, while the ion MCP is at 20°. The backscattering angle at the center of the ion MCP is 164°, so this plate is tilted 4° away from being perpendicular to the average backscattered path. This optimization of the angles is important for adapting the TOF approach to a large solid angle.

Figure 2 shows a feature in the research system which will also be incorporated into at least one of the detectors on the SEMATECH HIBS system. The ion MCP is mounted on a linear feedthrough such that it can be retracted 15 cm, thereby doubling the flight path. This allows trading sensitivity (solid angle) for somewhat improved mass resolution in specific experiments. Additionally, by changing to a lighter ion beam such as He, the system can be used in this longer flight path mode for relatively high resolution depth profiling near the surface, rather than high sensitivity. The solid angle for the MCP in the short flight path is 34 msr, while for the long flight path it is 11 msr.

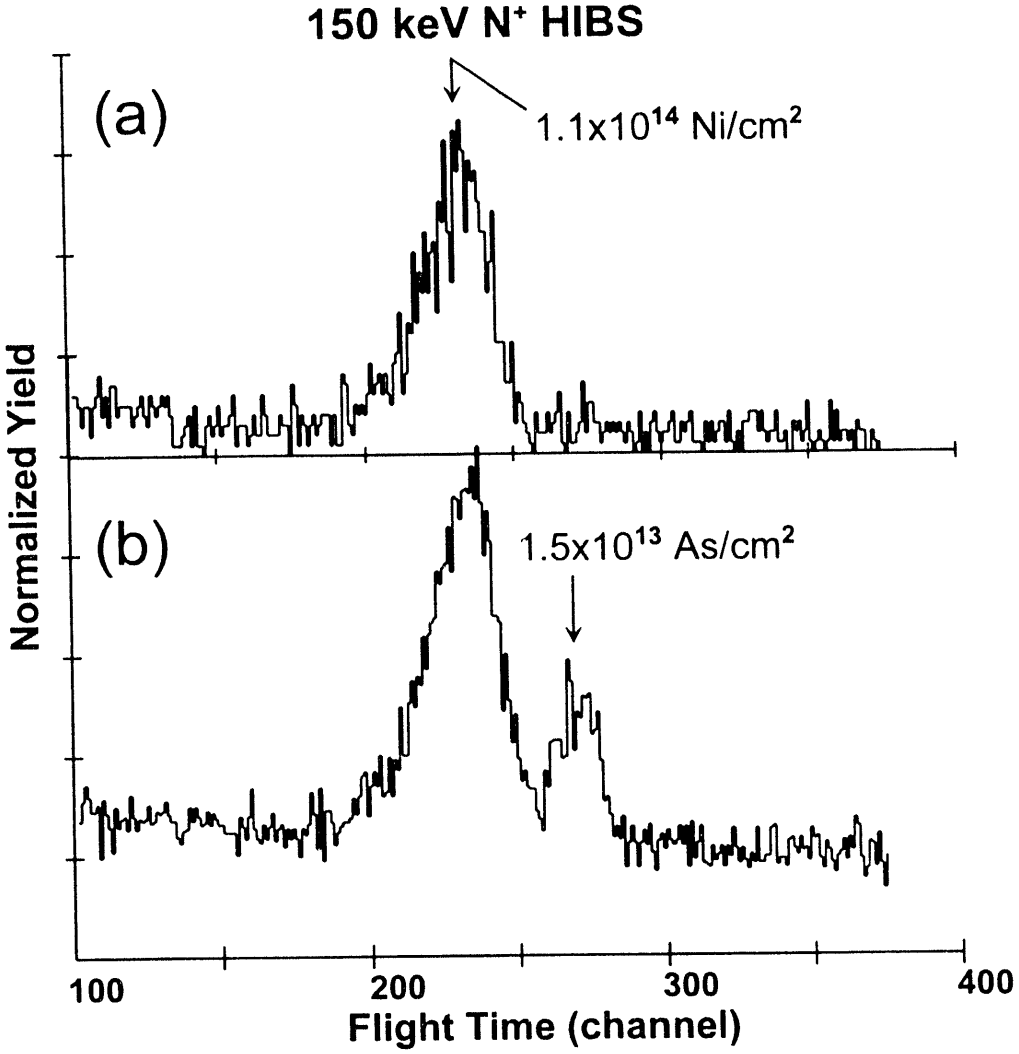

Figure 3. Spectra obtained (a) before, and (b) after installing a refurbished ion pump on the analysis chamber. Both spectra obtained from Ni-dosed Si under similar conditions.

APPLICATION EXAMPLES

The first example shown here is from a series of spectra taken during the installation and initial optimization of the TOF detector in a new analysis chamber. At one point in this process, a larger ion pump was installed under the main chamber in an effort to reduce the base pressure in the system. This pump was not newly manufactured, but a "refurbished" unit, thoroughly cleaned by the vendor but with an unknown history. Figure 3 shows two spectra obtained with 150 keV N^+ from a Si wafer deliberately contaminated with $1x10^{14}$ Ni/cm^2. Spectrum (a) is from before the pump addition, while (b) is after. Differences in background are due to differences in the electronic setup of the channelplates, but the most important difference is the addition of a peak near channel 280. This peak corresponds to $1.5x10^{13}$ atoms/cm^2 of As contamiantion, while the peak near channel 230 in each spectrum is due to the expected $1x10^{14}$ Ni/cm^2.

Figure 4 demonstrates that As was building up on the samples during the process of HIBS analysis. These spectra were also obtained with 150 keV N^+, but from a sample with a nominal dosing of $2x10^{12}$ Ni/cm^2. The dashed curve was collected with 50 μC of beam exposure, and then the second, solid curve was collected with an additional 50 μC on the same spot for a total exposure to the beam of 100 μC. Clearly, the As was building up with the beam exposure. The $1.2x10^{13}$ As/cm^2 present after 50 μC is already enough to obscure the contribution from Ni, while after 100 μC the $2.6x10^{13}$ As/cm^2 present completely covers the Ni portion of the spectrum. The broad tail to lower channels (longer flight time) also suggests that some of the As was being recoil implanted by the beam into the substrate.

Continued investigation showed that As contamination was appearing on all samples inserted into the system after the refurbished pump was installed, at levels which would not have been noticed in an ordinary RBS experiment. A subsequent examination of the pump gasket with X-ray microanalysis in an electron microscope confirmed the presence of As. Elimination of the contamination required complete disassembly and a plasma cleaning of the chamber, followed by installation of a new pump. The lesson to be learned is that considerable caution should be exercised with used components when building systems intended for studies of these very low levels of contamination.

A final example is shown in Fig. 5, demonstrating the research system capability after the problems with As were corrected. This spectrum was taken during a study comparing different trace analysis techniques, wherein a series of samples were deliberately dosed with different

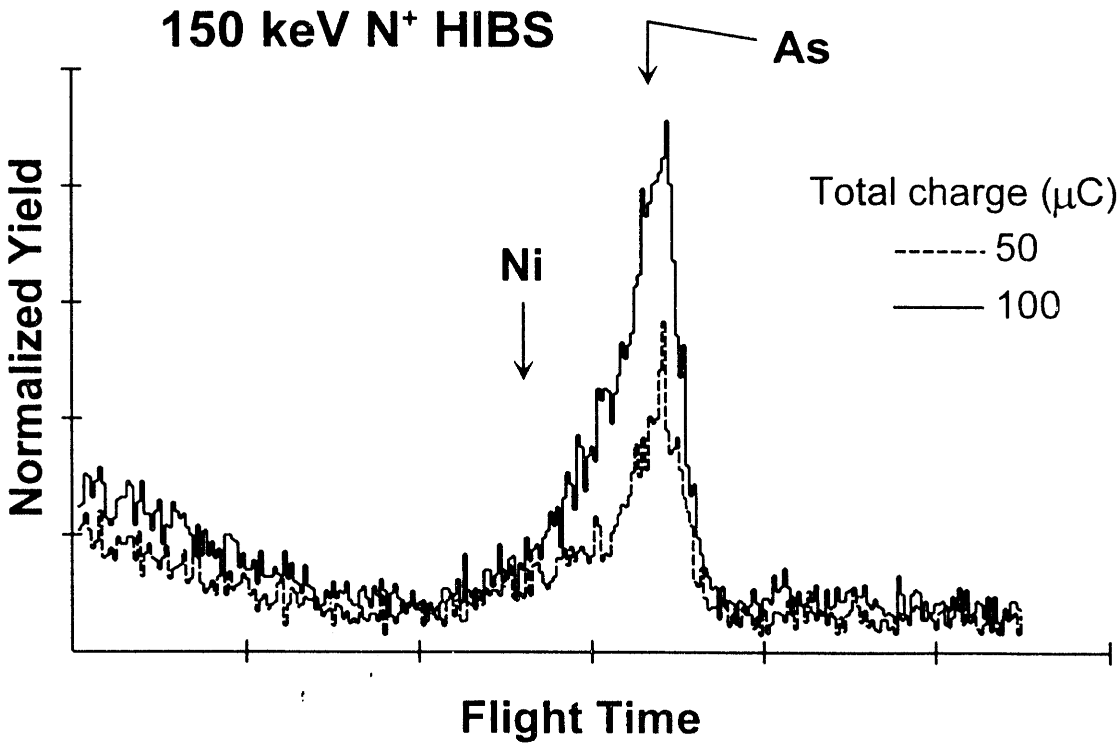

Figure 4. Two spectra sequentially obtained from the same spot on a Ni-dosed Si surface, running with a "refurbished" ion pump. Each was collected using 50 μC, for a total of 100 μC. The As contamination increases with beam exposure.

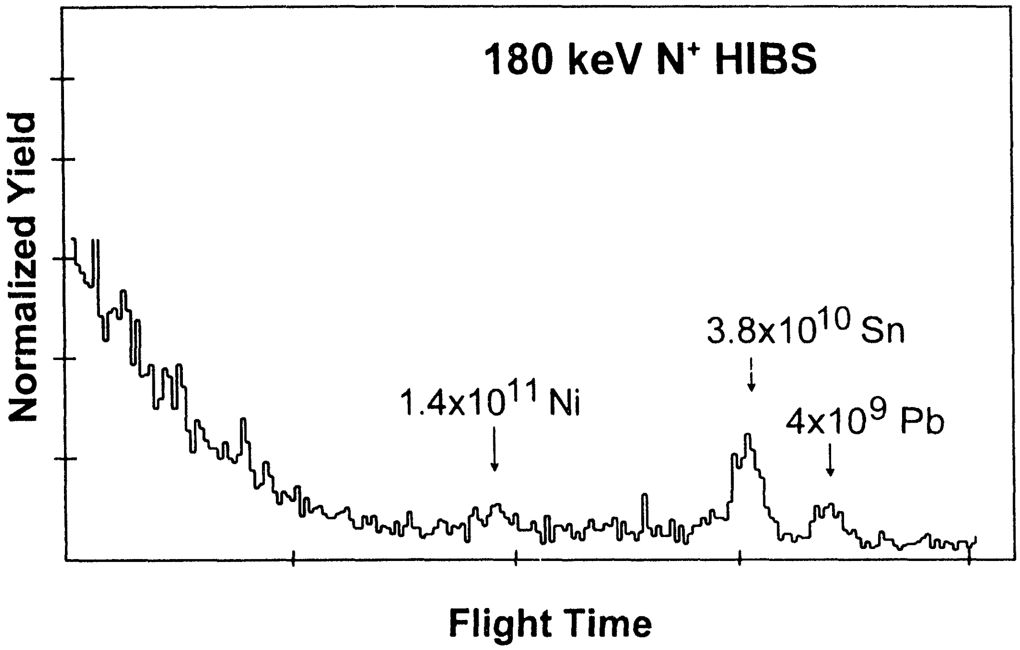

Figure 5. TOF-HIBS spectrum obtained from Si wafer contaminated with Ni, Sn and Pb.

levels of Ni, using an ashed photoresist. [11] The nominal dose for the sample shown in Fig. 5 was $1.5x10^{11}$ Ni/cm^2. HIBS analysis confirms the expected level of Ni and also demonstrates that the sample was contaminated with levels of Sn and Pb below the capability of TXRF. A subsequent examination using VPD followed by ICP-MS[12] showed that these low levels of Sn and Pb were indeed present on the wafers.

SENSITIVITY

The sensitivity of HIBS can be increased in a number of ways: increasing the solid angle by using multiple detectors in parallel, using a larger beam spot, channeling the incident beam along a crystal axis of the substrate, or using a higher Z, lower-energy beam. Of course, several factors affect the ultimate sensitivity which can be achieved. The efficiency of the channelplates for detecting electrons, ions and neutrals in this energy range is not well known, nor is the electron-producing efficiency of the ranging foil. The channelplates also have a count rate limitation which may in turn limit the amount of beam current which can be used. Multiple scattering in the target, where particles undergo several small angle scattering events and exit the sample with higher energy than a single large-angle event would produce, is expected to produce a background at low levels [13] and may be part of the observed background. Random coincidences (which have a similar effect on a TOF spectrum to pulse pileup in an energy spectrum) are largely eliminated by the range-timing foil, but because of energy straggling and non-uniformities in this foil, some particles scattered from the substrate come through the foil, producing a background at lower flight time and a small amount of random coincidences. Straggling in the foil also has a serious effect on resolution, dominating the observed time resolution and limiting the mass resolution that can be achieved. Furthermore, scattering in the foil results in some ions exiting at angles which don't intercept the ion channelplate, reducing the effective solid angle of the detector. This effect is worse at lower energy, eventually offsetting the gains in sensitivity that can be obtained by going to lower beam energy.

Sputtering of the sample surface by the analysis beam is the ultimate limit to the statistics which can be obtained, and hence the sensitivity. The rate of sputtering will depend on the state of the impurity: particles will sputter differently than widely dispersed, low concentration layers, so it is difficult to predict the limit in advance. Preliminary experiments measuring the rate of sputtering during HIBS analysis suggest that the rate for a sub-monolayer impurity is lower than predicted by a simple sputtering model using bulk sputtering rates.

The sensitivity of the research system in its present, single detector configuration ranges from ~5x10^{10} atoms/cm^{2} for Fe to ~1x10^{9} atoms/cm^{2} for Au, both for a Si substrate. Figure 6 compares the sensitivity of the prototype to that of TXRF, along with the expected sensitivity of the SEMATECH HIBS system. The latter, with three parallel detectors, optimized foils and a larger beam spot, should reach sensitivities of ~5x10^{9} atoms/cm^{2} for Fe and ~1x10^{8} atoms/cm^{2} for Au. The figure shows sensitivity scales with and without pre-concentration by VPD. The examples we have shown here illustrate that even though the elemental identification capability of HIBS (i.e., mass resolution) is not as good as other techniques such

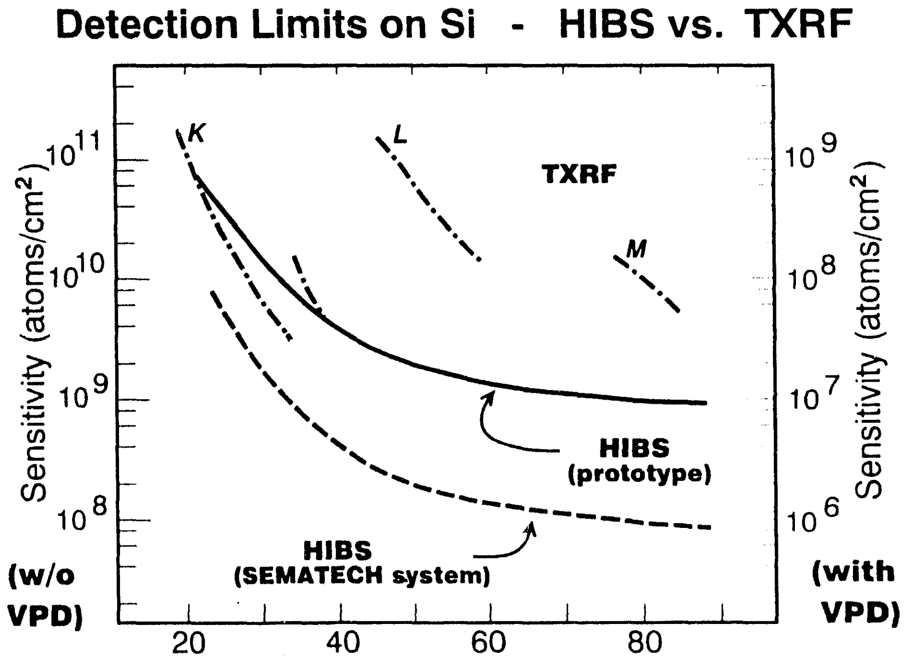

Figure 6. Detection limits for contaminants on Si. The solid line is the demonstrated sensitivity for the research HIBS prototype, while the dashed line is the anticipated sensitivity for the SEMATECH HIBS system, with three parallel detectors and a larger beam spot. Approximate sensitivities for TXRF are also plotted for comparison.

as TXRF, the lack of matrix effects and general sensitivity to all elements above Ar makes the technique very powerful.

ACKNOWLEDGMENTS

Technical assistance by D. L. Buller and K. G. Minor is gratefully acknowledged. The collaborations of B. L. Doyle and C. P. Resnick of Sandia Labs have been essential. This work was performed at Sandia National Laboratories and supported by the U.S. Department of Energy under contract no. DE-AC04-94AL85000.

REFERENCES

[1] B. L. Doyle, J. A. Knapp, and D. L. Buller, Nucl. Inst. and Meth. B42 (1989) 295.

[2] J. A. Knapp and B. L. Doyle, Nucl. Inst. and Meth. B45 (1990) 143.

[3] J. A. Knapp and J. C. Banks, Nucl. Inst. and Meth. B79 (1993) 457.

[4] J. A. Knapp, J. C. Banks, and B. L. Doyle, Nucl. Inst. and Meth. B85 (1994) 20.

[5] J. A. Knapp, J. C. Banks, and B. L. Doyle, Sandia National Laboratories internal report, SAND94-0391, (in press).

[6] See the other papers of this conference.

[7] M. Meuris, M. Heyns, W. Kuper, S. Verhaverbeke, and A. Philipossian, ECS, Washington, D. C., May 1991 (unpublished).

[8] E. Rutherford, Phil. Mag. 21 (1911) 669.

[9] C. G. Darwin, Phil. Mag. 28 (1914) 499.

[10] M. H. Mendenhall and R. A. Weller, Nuc. Inst. and Meth. B47 (1990) 193.

[11] W. F. Calaway, S. R. Coon, M. J. Pellin, D. M. Gruen, M. Gordon, A. C. Diebold, P. Maillot, J. C. Banks, and J. A. Knapp, Surface and Interface Analysis 21 (1994) 131.

[12] Unpublished data, J. Bayliss, SEMATECH.

[13] D. K. Brice, Nucl. Instr. and Meth. B69 (1992) 349.

DATE
FILMED
9/8/94

END